

# Double CD Nozzle Wind Tunnel Analysis

---

*Exploring Design Parameters under Closed-Loop,  
Supersonic Flow*

*Jonathan Yun & Andrew Ma*

11/22/2022

Ma, Yun	2
<b>Table of Contents</b>	
1.0 Introduction & Approach	3
1.1 Abstract	3
1.2 General Design	3
1.2.1 Summary	3
1.2.2 Justification	4
1.3 Problem Statement	4
1.4 Approach	5
1.4.1 Formulas	5
1.4.2 Statistical Methods	8
2.0 Results & Discussion	9
2.1 CD1 Throat to Test Section Height	9
2.2 CD2 Throat to CD1 Throat Height	10
2.3 Maximum Startup Power	10
2.4 Supersonic Inlet Temperature	11
2.5 Wedge Shock Angle	12
2.6 Surface Pressure to Upstream Pressure	13
2.7 Temperature Downstream of Wedge Shock	15
3.0 Conclusions	16
3.1 Explaining the Cost	16
3.2 Power Cost	16
3.3 Structural/Material Cost	16
Sources	17

## 1.0 Introduction & Approach

### 1.1 Abstract

We have been tasked with aiding in the design of a supersonic, closed-circuit, wind tunnel. The span of the wind tunnel is constant but its height varies over the test section and two converging-diverging nozzles. The two CD sections are connected to compressors and heat exchangers to ensure steady operating conditions.

Our sponsors would like to know how this wind tunnel would operate under three varying conditions: the working fluid, the test-sections Mach number, and the test-sections inlet stagnation temperature. Furthermore, the tunnel will be used to study flow over model shapes. We have been asked to analyze a wedge with an  $18^\circ$  apex angle. As the problem statement is investigated, the effects of the design space - namely, start up power, nozzle geometry, and the wind tunnel's structure, material, and insulation ability - have a direct relationship with the cost of construction and operation.

### 1.2 General Design

#### 1.2.1 Summary

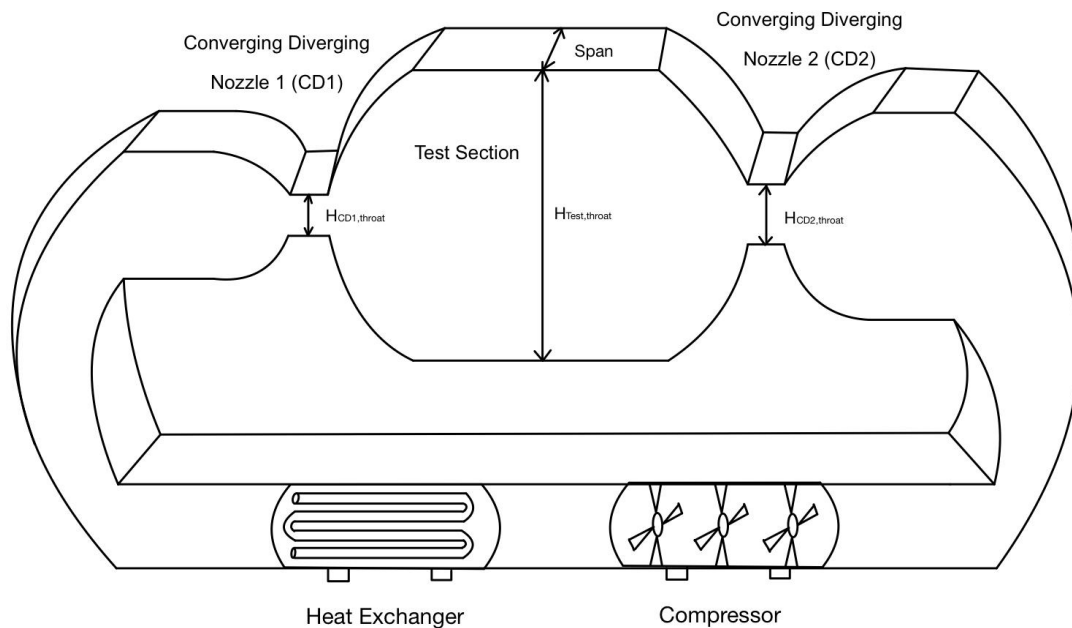


Figure 1

As demonstrated in *Figure 1*, the wind tunnel will follow a closed-loop design. The fluid will flow through the wind tunnel itself and be routed through a compressor, heat exchanger device, then back into the inlet of CD1. No fluid will be lost during operation.

The test section will have a square cross-section, implying that the span will equal the height of the test section.

### **1.2.2 Justification**

There are two fundamental design choices, both a consequence of the closed-return system, that we felt required context: the use of two converging-diverging nozzles and the addition of the compressor/heat exchanger network.

Given that the wind tunnel must sustain steady supersonic flow, the second nozzle must be configured to perform two major tasks: swallow the shock that starts in the test section as the flow approaches supersonic and keep the shock past its throat (so the shock isn't susceptible to shifting back into the test section) and before its exit (so the compressor and heat exchanger doesn't absorb the shock). The effectiveness of the nozzle will be solely determined by the height (and thus the area) of the nozzle throats and test section.

The compressor's function is to manipulate the pressure difference between the ends of the tunnel to start, increase, and maintain the fluid's velocity in the wind tunnel. The temperature of the fluid (which increases as the compressor does work to it), is controlled by the heat exchanger that follows the compressor.

With the compressor, heat exchanger, and configuration of the nozzles working in tandem, we can cleverly optimize the closed-loop system and highlight its major advantage: power savings. The compressor requires a marginal amount of power to maintain supersonic operation, and the power cost of this system will arise only during startup (a quantity that will be solved for in Section 2.3) and going between velocities when needed during operation. When compared to an open wind tunnel, the closed system is more efficient, albeit more complex [1].

## **1.3 Problem Statement**

The design space is composed of 3 parameters that will be examined in this analysis:

1. Working fluid. The tunnel will operate using only air, helium, or nitrous oxide in their gaseous forms.
2. Test section Mach number. While the Mach number of the fluid can vary at different points in the wind tunnel, the operational Mach number of the fluid in the test section will be controlled over a range of 1.5-4.5, thus classifying this system as a supersonic wind tunnel.
3. Test section inlet stagnation temperature. Similarly to the Mach number, the stagnation temperature will inevitably vary at different points in the wind tunnel, but the stagnation temperature of the inlet of the test section will be controlled over a range of 260-700 K.

For operation without a model mounted in the test section, we have calculated the following tunnel design aspects over the 3 design parameters:

1. Height ratio of the CD1 throat to the test section (see *Figure 1*).
2. Height ratio of the CD2 throat to CD1 throat required to start the wind tunnel and output optimal stagnation pressure loss
3. Normalized maximum power of the compressor [reference] required to start the tunnel
4. Static temperature at the inlet of the test section as the tunnel operates with steady, supersonic flow

For operation with a wedge (apex angle  $\alpha = 18^\circ$ ) mounted in the test section, we have calculated the following tunnel design aspects over the 3 design parameters:

5. The shock angle off the wedge during supersonic operation
6. Static pressure ratio of the wedge surface to the upstream static pressure of the test section
7. Static temperature downstream of the shock that omits off the wedge

## 1.4 Approach

### 1.4.1 Formulas

#### 1.4.1.1 Throat Ratio of CD 1 to the Test Section Height [Eqn 1]

$$\begin{aligned}
 H_{\text{throat}}^2 &= A_{\text{test}} \quad \text{solve for } \frac{H_{\text{throat}}}{H_{\text{test}}} \\
 H_{\text{throat}}^2 &= A_{\text{throat}} = A^* \quad (\text{choked at nozzle}) \\
 \frac{A_{\text{throat}}}{A^*} &= \frac{H_{\text{throat}}^2}{H_{\text{throat}}^2} = \frac{1}{M} \left( \frac{1 + \frac{\gamma-1}{2} M^2}{\frac{\gamma+1}{2}} \right)^{\frac{\gamma+1}{2(\gamma-1)}} \\
 \frac{H_{\text{throat}}}{H_{\text{test}}} &= \sqrt{\frac{1}{\frac{1}{M} \left( \frac{1 + \frac{\gamma-1}{2} M^2}{\frac{\gamma+1}{2}} \right)^{\frac{\gamma+1}{2(\gamma-1)}}}}
 \end{aligned}$$

### 1.4.1.2 Throat Ratio Height of CD 2 to CD 1 to Start Tunnel and Have Minimum Stagnation Pressure Loss [Eqn 2]

$$\left. \frac{A_{c02}}{A_{c01}} \right|_m \sim \left. \frac{P_{01}}{P_{02}} \right|_m$$

$$\frac{P_{02}}{P_{01}} = \left[ \frac{\frac{\gamma+1}{2} M^2}{1 + \frac{\gamma-1}{2} M^2} \right]^{\frac{\gamma}{\gamma-1}} \left[ \frac{2\gamma}{\gamma+1} M^2 + \frac{\gamma-1}{\gamma+1} \right]^{\frac{1}{2}(\gamma-1)}$$

$$\sqrt{\frac{A_{c02}}{A_{c01}}} = \sqrt{\frac{1}{\left[ \frac{\frac{\gamma+1}{2} M^2}{1 + \frac{\gamma-1}{2} M^2} \right]^{\frac{\gamma}{\gamma-1}} \left[ \frac{2\gamma}{\gamma+1} M^2 + \frac{\gamma-1}{\gamma+1} \right]^{\frac{1}{2}(\gamma-1)}}}} = \frac{H_{cd2}}{H_{cd1}}$$

### 1.4.1.3 Normalized Maximum Compressor Power to Start Tunnel [Eqn 3]

Solve for  $\frac{\dot{W}}{P_{01} (H_{thrust})^2}$

specific work  $w = h_{02} - h_{01} = c_p (T_0 - T)$

$$\frac{T_0}{T} = \left( \frac{P_0}{P} \right)^{\frac{\gamma-1}{\gamma}}$$

$$w = c_p T_0 \left[ \left( \frac{P_0}{P} \right)^{\frac{\gamma-1}{\gamma}} - 1 \right]$$

$$w \dot{m} = \dot{W} \quad \dot{m} = \rho v A = \rho M \sqrt{\gamma R T_0} H^2$$

$$\frac{\dot{W}}{\rho H^2} = \frac{\dot{W}}{\rho R T_0 H^2} = \frac{c_p T_0 \left[ \left( \frac{P_0}{P} \right)^{\frac{\gamma-1}{\gamma}} - 1 \right] \rho M \sqrt{\gamma R T_0} H^2}{\rho R T_0 H^2}$$

$$= \frac{c_p \left[ \left( \frac{P_0}{P} \right)^{\frac{\gamma-1}{\gamma}} - 1 \right] \sqrt{\gamma R T_0} M}{\sqrt{R}}$$

$$= \frac{\frac{\gamma}{\gamma-1} \left[ \left( \frac{P_0}{P_2} \right)^{\frac{\gamma-1}{\gamma}} - 1 \right] \sqrt{\gamma R T_0} M}{\sqrt{R}} = \frac{\gamma^{1/2} M T_0^{1/2} \gamma^{1/2} \left[ \left( \frac{P_0}{P_2} \right)^{\frac{\gamma-1}{\gamma}} - 1 \right]}{\gamma-1}$$

#### 1.4.1.4 Static Temperature at Inlet during Steady, Supersonic Operation [Eqn 4]

$$\frac{T_0}{T} = 1 + \frac{\gamma-1}{2} M^2$$

$$T = \frac{T_0}{\left(1 + \frac{\gamma-1}{2} M^2\right)}$$

$$T(T_0, M) = \frac{T_0}{\left(1 + \frac{\gamma-1}{2} M^2\right)}$$

#### 1.4.1.5 Shock Angle off Wedge [Eqn 5]

$$1.5 \leq M_1 \leq 4.5, \quad \delta = \frac{1}{2}(18^\circ) = 9^\circ, \quad \alpha = 1 \text{ (weak shock)}$$

$$\lambda = \sqrt{(M_1^2 - 1)^2 - 3 \left(1 + \frac{\gamma-1}{2} M_1^2\right) \left(1 + \frac{\gamma+1}{2} M_1^2\right) \tan^2 \delta}$$

$$X = \frac{1}{\lambda^3} \left[ (M_1^2 - 1)^3 - 9 \left(1 + \frac{\gamma-1}{2} M_1^2\right) \left(1 + \frac{\gamma-1}{2} M_1^2 + \frac{\gamma+1}{4} M_1^4\right) \tan^2 \delta \right]$$

$$\theta = \tan^{-1} \left[ \frac{M_1^2 - 1 + 2\lambda \cos\left(\frac{4\pi\alpha + \cos^{-1}X}{3}\right)}{3 \left(1 + \frac{\gamma-1}{2} M_1^2\right) \tan \delta} \right]$$

#### 1.4.1.6 Ratio of Static Pressure on to Upstream of Wedge [Eqn 6]

$$\frac{p_2}{p_1} = \frac{p_2}{p_1} = \frac{2\gamma}{\gamma+1} M_1^2 \sin^2 \theta - \frac{\gamma-1}{\gamma+1}$$

$$p_2 = \text{on wedge} \quad p_1 = \text{upstream}$$

#### 1.4.1.7 Static Temperature Downstream of Shock [Eqn 7]

$$\frac{T_2}{T_1} = \frac{\left(1 + \frac{\gamma-1}{2} M_1^2 \sin^2 \theta\right) \left(\frac{2\gamma}{\gamma-1} M_1^2 \sin^2 \theta - 1\right)}{M_1^2 \sin^2 \theta (r+1)^2 / 2(\gamma-1)}$$

$T_2 = \text{downstream} \quad T_1 = \text{upstream}$

#### 1.4.2 Statistical Methods

Since we used the aforementioned formulas over a range of test section Mach numbers and test section inlet stagnation temperatures, most of our results were also a range of values, requiring either an array or graph to represent their relationship with the design space. From a computation standpoint, this requires creating vectors of arbitrary length and spacing to be used as variables in our MATLAB code.

In order to maintain statistical integrity, we wanted to ensure that our results shown in this report were calculated over Mach and stagnation temperature vectors with a sufficient level of precision. Additionally, we wanted our code to be reusable for applications of varying precision requirements. For example, if a user wanted to quickly understand the trend between maximum startup compressor power and the mach range, they could easily output a readable vector of 4 values of power over a mach range of 1.5, 2.5, 3.5, and 4.5. On the other hand, if the user wants an extremely comprehensive graph, they can pull results by iterating over, for example, every thousandth Mach number and stagnation temperature in the specified range.

To achieve this user flexibility, we employed a for loop to create Mach and stagnation temperature vectors with a variable “precision” that determines the length and iteration of the vectors. The vectors are cleared after every time the scripts are run.

```

1 - precision=10;
2 - step=3/precision;
3 - mach = zeros(1, precision);
4 - mach(1) = 1.5;
5 - for i=2:precision+1
6 -     mach(i)=mach(i-1)+step;
7 - end
8 - %Mach vector with adjustable precision

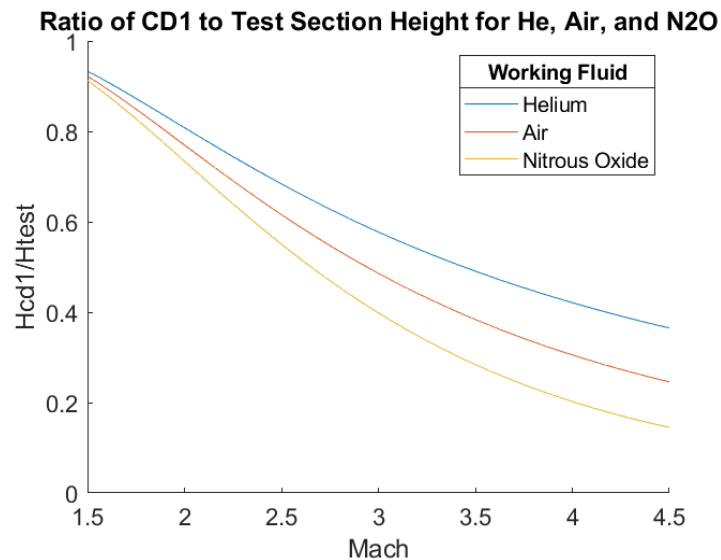
```



We decided on using a precision of 100 for the results you will see in this report. This value will create a Mach and stagnation temperature vector of length 101, outputting a result (for example, the height ratio of the CD1 throat to the test section) of length 101.

## 2.0 Results and Discussion

### 2.1 CD1 Throat to Test Section Height

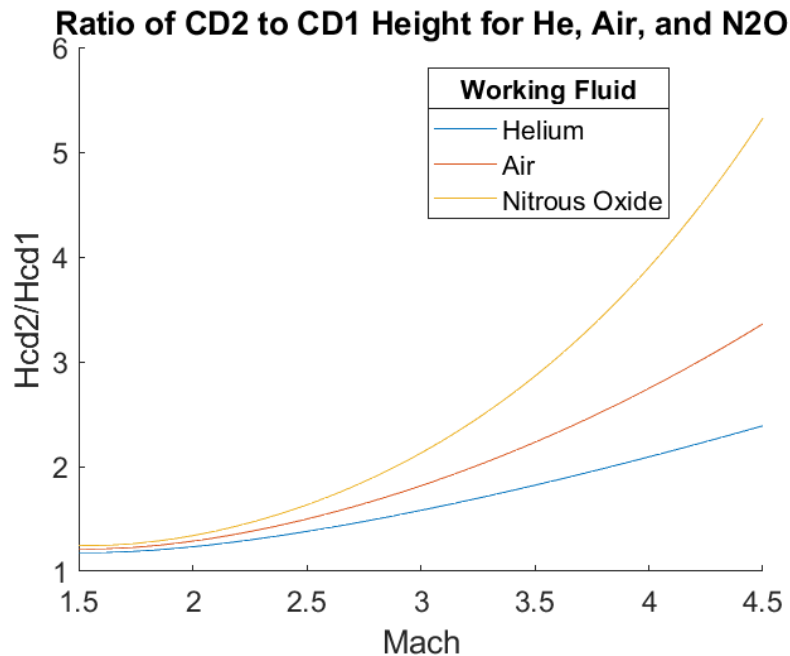


Over a Mach range of 1.5-4.5 for helium, air, and nitrous dioxide, we see that the ratio of the first CD nozzle height to the height of the test section decreases with increasing mach number. This aligns with what we know about how diverging nozzles can increase the speed of a fluid pass sonic. If the ratio were greater than 1, it would still be a converging nozzle slowing flow, and if it were equal, speed would not increase unless back pressure was somehow constantly decreasing.

Another interesting thing to note is the relation between these three different fluids. N2O decreases slightly more rapidly than air which decreases slightly more rapidly than helium. The findings align with the only variable between these three fluids which is their specific heat ratio or isentropic expansion factor. A larger specific heat ratio results in less expansion at higher speeds. Using the stagnation density equation, we can see that a higher specific heat ratio will result in a smaller change in density. This means that fluids with higher specific heat ratios take up less space for the same amount of mass after the fact. Helium has the highest specific heat ratio of 1.6, with air following at 1.4 and N2O at 1.22. Assuming the same amount of mass flow, the ratio of the throat to test section height for helium should be the closest to 1 because it has the highest specific heat ratio of the three. On the other hand, N2O's ratio of throat to test

section height should be smaller because a larger test section height is required for its expansion compared to helium, and we see that this is also true.

## 2.2 CD2 Throat to CD1 Throat Height



In the windtunnel, the test fluid goes from being choked, to supersonic in the test section, and then finally goes through the second CD nozzle. From the Section 2.2 graph, we see that the ratio of heights of CD2 to CD1 is nearly the inverse of the ratio of the height of CD1 to the test section height. From this, we can determine that the height of the second throat will be very close to that of the test section height. It can also be seen that the ratio in this graph increases with increasing mach. Since we want the tunnel to start and have minimum stagnation pressure loss, the second nozzle should not do anything to increase the speed of the fluid which would increase the stagnation pressure loss. The second CD nozzle should be there to slow the speed enough to reduce the stagnation pressure loss, but at the same time, not allow for supersonic flow past the throat. For the same reasoning as Section 2.1, we see that N<sub>2</sub>O has the largest second nozzle height ratio followed by air then helium.

## 2.3 Maximum Startup Power

For this section, we used energy conservation and assumed that the wind tunnel system is insulated (thus adiabatic) and experiences steady flow. Furthermore, we took the time derivative and normalized our findings for maximum start up work for the sake of comparison between the

three working fluids. By dividing the work rate by the force exerted by the fluid in the test section, we account for area differences created by the unique working fluids.

Using Eqn 3 over our design space (stagnation temperature, mach range) with the specific heat capacities and gas constants [2] of helium, air, and nitrous oxide, we created a vector of start up work and took the maximum value from each vector, yielding (in descending order):

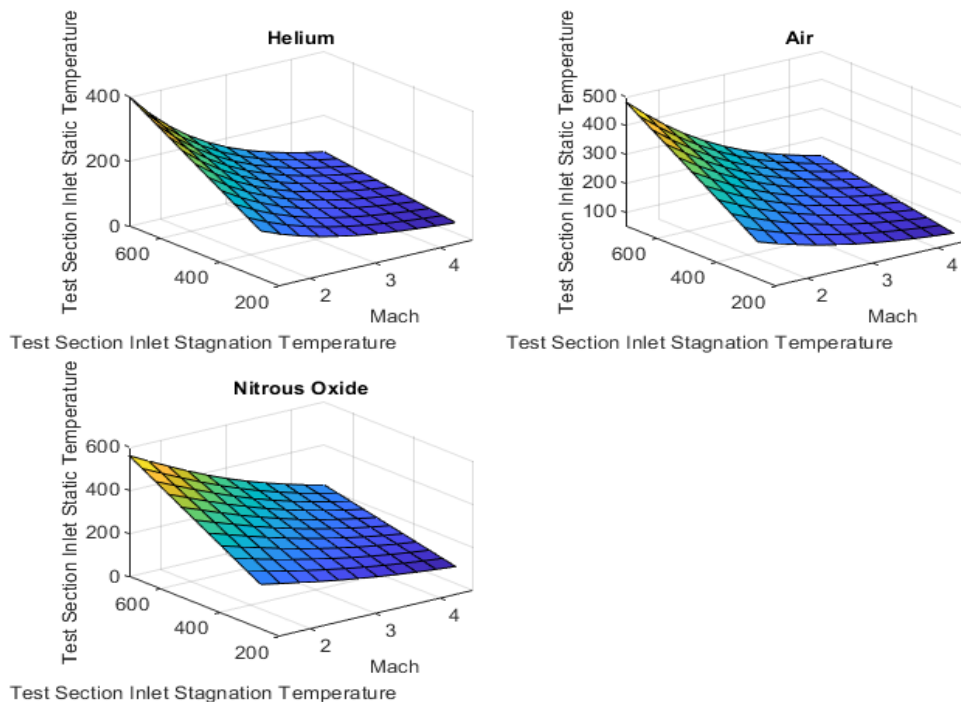
$8.27 \times 10^2$  m/s as the maximum value for nitrous oxide

$5.39 \times 10^2$  m/s as the maximum value for helium

$4.57 \times 10^2$  m/s as the maximum value for air

As stated in Section 1.2.2, the work done by the compressor to start up and maintain flow in our system is not linear. The closed loop design allows an “upfront” amount of compressor work to provide both the work needed to start the tunnel and most of the work required to sustain supersonic operation. We will refer to this “upfront” work as “startup” work. The fluid, which starts at rest, is accelerated by a pressure difference between the entrance of CD1 and exit of CD2. The pressure of the fluid at the entrance of CD1, hereinafter referred to as  $p_o$ , is raised using the compressor, initially creating subsonic flow everywhere in the system. Eventually,  $p_o$  can be raised sufficiently above the wind tunnel’s back pressure,  $p_b$ , to achieve supersonic flow in the system. After the shocks have been swallowed by the throats of CD1 and CD2, the compressor must only make up the marginal pressure losses in the system made by turns or system inefficiencies.

## 2.4 Supersonic Inlet Temperature



Since static temperature is both a function of mach number and stagnation temperature, a 3D surface map is required to visualize the effects of stagnation temperature and mach on the static temperature at the inlet to the test section. In this adiabatic system where energy is conserved, the only way for the fluid to gain kinetic energy is to transfer from thermal energy and vice versa. We see that at the extreme of high stagnation temperature and low mach, static temperature reaches a maximum. At the other side of the spectrum where stagnation temperature is low and mach is high, static temperature reaches a minimum. If we were to look at this graph from a 2D view with constant mach, we see that static temperature increases linearly with an increase in stagnation temperature which holds true to the stagnation temperature equation:

$$T = \left( \frac{1}{1 + (k-1) \times \frac{M^2}{2}} \right) T_o$$

On the other hand, if we were to hold stagnation temperature constant, there is an exponential relation between mach and static temperature which can also be seen in the stagnation temperature equation.

Comparing the three different fluids, we see that nitrous oxide has the steepest slopes compared to that of helium and air. The lower specific heat ratio creates a more lower reaction to changes in temperature resulting in a much smoother slope compared to the others.

## 2.5 Wedge Shock Angle

Since we know that the speed of the fluid in the test section just before hitting the wedge is supersonic, an oblique shock must be formed at the surface of the wedge. In this section, we calculated the shock angle of this oblique shock, demonstrated in *Figure 2*.

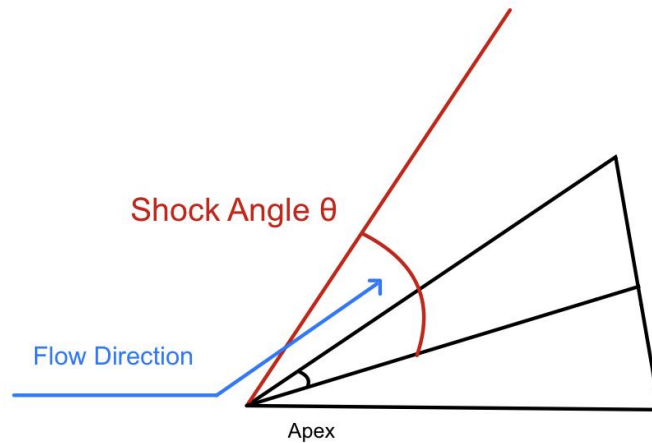
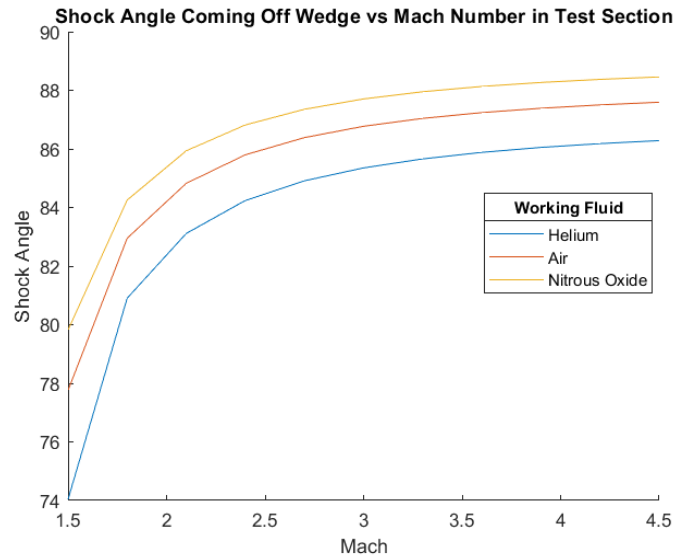


*Figure 2*

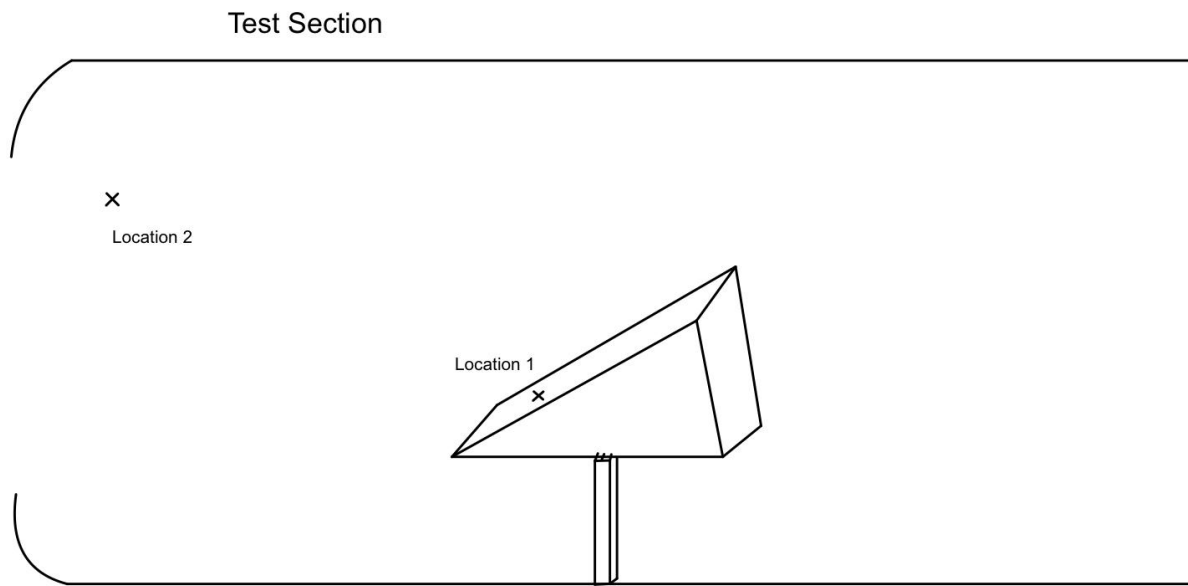
In our calculation, the shock angle equation we utilized has both a strong and weak shock solution ( $\alpha$  shown in Eqn 5). Assuming the volume of the test section is significantly larger than the volume of the wedge mounted inside, a weak shock solution would be appropriate for this application. The strength of the shock has a negligible relationship with the physical casing of the test section, as the pressure at a point far from the wedge is essentially the static pressure at that point.



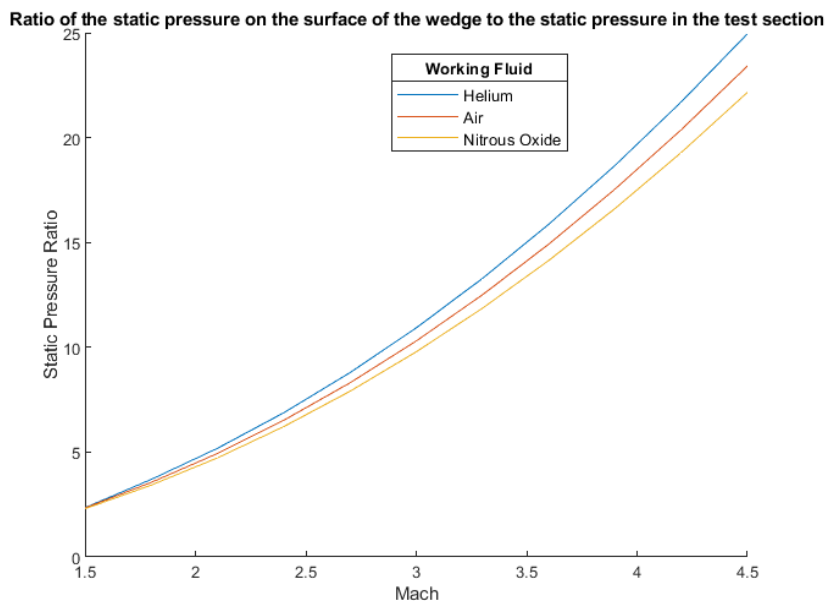
While the shock angle varied drastically in the lower range of Mach numbers, the angle is shown to approach around  $88^\circ$  and plateaus in growth starting around Mach 2.5. The working fluids experienced a consistently varying relationship with helium starting and ending with the lowest shock angle and nitrous oxide starting and ending with the highest.

## 2.6 Surface Pressure to Upstream Pressure

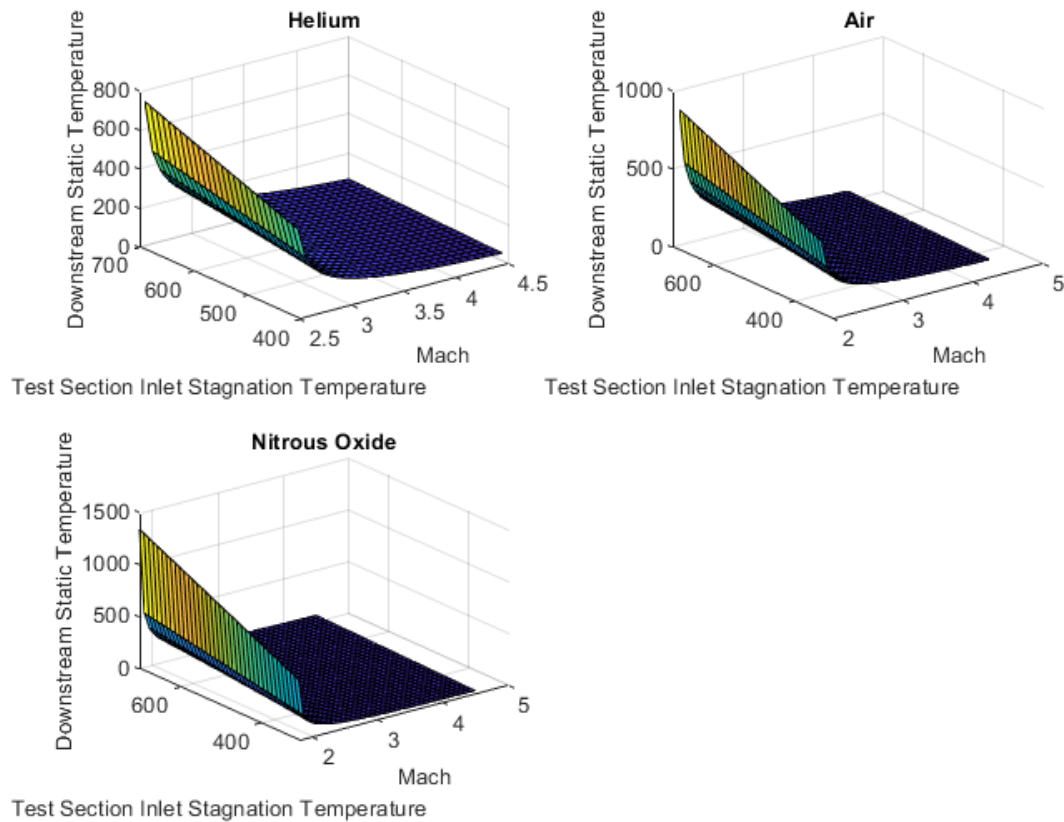
Our sixth task was computing the ratio of the static pressure on the surface of the wedge (Location 1 in *Figure 3*) with the static pressure far upstream in the test section (Location 2 in *Figure 3*) during supersonic operation. As alluded to in the previous section, the static pressure far upstream is not affected by the oblique shock on the wedge, making the pressure difference an important measurement for the structural design of the wind tunnel and understanding of how the pressure at the wedge varies between the different working fluids.

*Figure 3*

At the lower end of the Mach range, the working fluid has a negligible effect on the difference in static pressure from the surface to the upstream flow. At Mach 1.8, the difference between the highest and lowest pressure ratios (nitrous oxide, helium) is only 2.22%. By Mach 2.4, this difference rises to 9.61%, and by Mach 4.5 (end of our range), the difference is at 11.1%, where pressure differences now have a noticeable effect on the structure of the wind tunnel.



## 2.7 Temperature Downstream of Wedge Shock



These graphs show that downstream static temperature increases with an increase in inlet stagnation temperature and a decrease in Mach. The findings for this section are very similar to Section 2.4 as in when we hold Mach constant, there is a positive linear relationship between inlet stagnation temperature and downstream static temperature. Looking at Eqn 7 from section 1.3.1.7, we see that for a given Mach and shock angle, the downstream static temperature is just the stagnation temperature multiplied by a constant. Also, much like the other graph, with increasing Mach, more thermal energy is converted into kinetic energy, accounting for the decrease in static temperature as Mach goes up.

One way in which this section differs from 2.4 is that the three graphs decrease more rapidly. Since both sections have an exponential Mach in them, this significant decrease is likely due to the addition of an exponential sinusoidal function. This sinusoidal function would be the result of adding in a wedge, and if we were to add a steeper wedge, the graphs would likely have an even steeper slope.

## **3.0 Conclusions**

### **3.1 Explaining the Cost**

Ultimately, the cost of supersonic operation is largely affected by the power required to start and maintain the supersonic flow and the structural support and choice of material. Both of these factors have a direct, inverse relationship with the cost of operation. As proven in this report, our design space is the driving, if not sole, influencer of start up power and test section design. This conclusion will serve to “bottom line” our findings with the financial perspective in mind.

### **3.2 Power Implications**

If operating the windtunnel using ambient air, the wind tunnel’s wall experiences 457 watts per pressure per square meter. Depending on the size and pressure you’d like to operate the wind tunnel at, this number can stack up to be a lot when used for prolonged periods of time. Say you wanted to put a rectangular wing with a span of 10 meters in the test section. This would multiply your required power usage by a factor of 100, and power usage only increases depending on your operating test section pressure. To run this wind tunnel you would consume 16,452 kilowatts of energy per hour. According to the U.S. Energy Information Administration, that is the equivalent of what the average home in Georgia uses for the entire year [3].

### **3.3 Structural/Material Implications**

When building this windtunnel, it is important to note which materials can withstand the inlet static temperature involved with supersonic operation as well as the downstream shock static temperature when testing model shapes in the wind tunnel. For common use with air at low mach, the test section inlet static temperature can reach up to roughly 500 degrees Kelvin. This suggests that materials used for the model shape should be able to withstand these types of temperature. As for downstream shock test section temperatures, make sure that the materials used to build the test section are suitable for operation at temperatures up to 1500 Kelvin depending on what fluid you are using. The reliability and longevity of the wind tunnel will ultimately depend on what materials you decide to use.

Furthermore, the choice of your working fluid affects the way the wind tunnel were to operate. As mentioned early, one implication of different working fluids is the maximum temperature at which they reach throughout the tunnel. For a good middle ground of low temperature, high mach, and low power startup, air would definitely be the best option. Not only that, but ambient air is widely available for use.



## Sources

[1] "Closed Return Wind Tunnel." NASA, NASA,

<https://www.grc.nasa.gov/www/k-12/airplane/tuncret.html>

[2] "Gases - Specific Heats and Individual Gas Constants." *Engineering ToolBox*,

[https://www.engineeringtoolbox.com/specific-heat-capacity-gases-d\\_159.html](https://www.engineeringtoolbox.com/specific-heat-capacity-gases-d_159.html).

[3] "Household Energy Use In Georgia." EIA,

[https://www.eia.gov/consumption/residential/reports/2009/state\\_briefs/pdf/ga.pdf](https://www.eia.gov/consumption/residential/reports/2009/state_briefs/pdf/ga.pdf)